



## Observations of Water Vapor Vertical Distribution by SPICAM/MEX and their Implications

Luca Maltagliati, Anna Fedorova, Franck Montmessin, Jean-Loup Bertaux, Oleg Korablev, Aurélie Reberac

### ► To cite this version:

Luca Maltagliati, Anna Fedorova, Franck Montmessin, Jean-Loup Bertaux, Oleg Korablev, et al.. Observations of Water Vapor Vertical Distribution by SPICAM/MEX and their Implications. Fourth International Workshop on the Mars Atmosphere: Modelling and Observations, Feb 2011, Paris, France. 5p. hal-00566574

**HAL Id: hal-00566574**

**<https://hal.science/hal-00566574>**

Submitted on 16 Feb 2011

**HAL** is a multi-disciplinary open access archive for the deposit and dissemination of scientific research documents, whether they are published or not. The documents may come from teaching and research institutions in France or abroad, or from public or private research centers.

L'archive ouverte pluridisciplinaire **HAL**, est destinée au dépôt et à la diffusion de documents scientifiques de niveau recherche, publiés ou non, émanant des établissements d'enseignement et de recherche français ou étrangers, des laboratoires publics ou privés.

# OBSERVATIONS OF WATER VAPOUR VERTICAL DISTRIBUTION BY SPICAM/MEX AND THEIR IMPLICATIONS

**L. Maltagliati**, *LATMOS, Guyancourt, France* ([luca.maltagliati@latmos.ipsl.fr](mailto:luca.maltagliati@latmos.ipsl.fr)), **A. Fedorova**, *IKI, Moscow, Russian Federation*, **F. Montmessin**, **J.-L. Bertaux**, **A. Reberac**, *LATMOS, Guyancourt, France*, **O. Korablev**, *IKI, Moscow, Russian Federation*.

## **The importance of H<sub>2</sub>O vertical distribution in the Martian water cycle:**

Since the first detection of water vapour by Spinrad et al. (1963), the water cycle of Mars has been studied almost exclusively through the analysis of nadir observations of water vapour column abundance. Other useful diagnostics have been neglected or only sparsely employed, mainly because of the technical difficulties of such measurements. Amongst them, the vertical distribution of water vapour is one of the most important. It allows to investigate the effective role of poorly constrained water sources and sinks, such as vertical atmospheric transport, water phase changes, surface-atmosphere exchanges, vertical redistribution associated with clouds. Information regarding the height of the saturation level, and consequently the temperature structure of the atmosphere and the formation of water ice clouds, can also be extracted. Related phenomena, such as delayed condensation, formation of ice particles, and deposition of water in the layers just below the saturation height, have never been observed but have a potentially significant impact on the water cycle, as demonstrated theoretically (Richardson et al. 2002, Montmessin et al. 2004). Finally, water is heavily involved in photochemical processes in the upper atmosphere that are still poorly constrained by observations (Krasnopolsky 2006, Lefèvre et al. 2008). The vertical distribution has also important consequences for the computation of the total column density, because it potentially accounts for a significant uncertainty of the integrated water abundance (e.g. Maltagliati et al. 2008).

In the history of Mars exploration before Mars Express, only one instrument managed to retrieve direct observations of the water vapour vertical profile: the ISM spectrometer on the Phobos-2 spacecraft. The results, presented by Rodin et al. (1997), probe the atmosphere between 10 and 50 km and reveal an altitude layer at  $\sim 25$  km with rapidly declining mixing ratio connecting two regions of almost constant concentration. However, the individual profiles exhibit significant scattering. Phobos-2 was active only for a limited amount of time, and the observations span less than one Martian month after the Northern spring equinox ( $L_s = 0^\circ - 20^\circ$ ) and a limited spatial coverage in the equatorial band. The conclusions by Rodin et al. (1997), thus, cannot be straightforwardly generalised for the whole planet at all seasons, and need to be confirmed by further

measurements. Furthermore, other indirect retrievals suggest a scenario where water vapour is less well-mixed (Davies 1979, Fouchet et al. 2007, Tschimmel et al. 2008).

Due to this scarcity of measurements, the vertical characterization of the atmosphere of Mars still depends heavily upon General Circulation Model predictions that employ strong assumptions needing measurement validation. A new and extensive dataset is provided by the SPICAM instrument.

## **The solar occultations by SPICAM/MEx:**

SPICAM is one of the spectrometers onboard the Mars Express spacecraft. It consists of two channels probing the ultraviolet (118 – 320 nm) and the near-infrared (1000 – 1700 nm) wavelength range with a spectral resolution of  $\sim 1$  nm. SPICAM is the only spectrometer on Mars Express that has a dedicated mode of observation in solar and stellar occultations.

The occultation technique is a commonly used technique for the vertical profiling of Earth and planetary atmospheres. A source of light (the Sun or a star) is observed through the atmosphere at different altitudes, and the resulting spectrum is ratioed with a reference solar spectrum observed outside the atmosphere. In this way only the signatures of atmospheric constituents remain. The main advantage of the occultation technique is its insensitivity to any instrumental effect. Moreover, since a new reference spectrum is collected with every new observation, it is not affected by instrumental ageing. On the negative side, the lowest atmospheric layers cannot be probed by the occultations, because the high dust loading of the atmosphere attenuates the signal and hides the spectral signatures.

For this study we use the SPICAM-IR channel in solar occultation mode. During its 7 years of activity, SPICAM has acquired more than 700 occultations, with a good seasonal and spatial coverage (Figure 1). Because the full IR wavelength range is scanned at full spectral resolution in 24 s., which is a too long time interval completely inappropriate for solar occultations, only a spectral window between 1350 and 1470 nm of the channel is retrieved at full resolution. This allows to reduce the acquisition time to 4 s. and still monitor simultaneously both water vapour and carbon dioxide (with the 1380 and 1430 nm bands respectively). In addition, ten continuum wavelengths throughout the full SPICAM-IR range are retrieved, in order to get information on the aero-

sol extinction. The vertical resolution varies with the orbit, from 2.5 to 7.5 km with an average of 4.5 km.

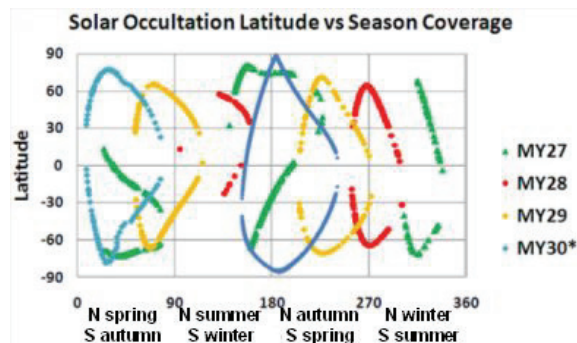


**Figure 1: four Martian Years of SPICAM solar occultations, from January 2005 to February 2011, with respect to Ls (season) on the x axis and latitude on the y axis.**

The transmittances derived from the spectral ratioing are fitted by a line-by-line spectral model and vertically inverted with a Levenberg-Marquardt procedure (with Tikhonov regularization) in order to retrieve the local density profile. The spectral information is extracted from the HITRAN 2004 database (Rothman et al. 2005) and the climatological parameters are taken from the Mars Climate Database (MCD 4.3, Millour et al. 2008) based on the General Circulation Model developed at the LMD laboratory (Forget et al. 1999). The detection limits are  $10^{10} \text{ cm}^{-3}$  for water vapour and few units in  $10^{11} \text{ cm}^{-3}$  for  $\text{CO}_2$ . The first results from SPICAM solar occultations (treated with a slightly different procedure) have been presented by Fedorova et al. (2009). The lowest probed altitude depends strongly on the atmospheric dust loading, and varies from 10 km for very clean conditions, found at aphelion in the southern hemisphere, up to 60 – 70 km in case of strong dust activities, which are more common during northern autumn.

Here we present the results for the two occultation campaigns of MY29. The first one is made up by 60 profiles around the aphelion season ( $L_s = 72^\circ$ ), covering the end of northern spring and beginning of summer ( $L_s = 50^\circ - 110^\circ$ ), while the second one includes  $\sim 70$  profiles during northern fall ( $L_s = 210^\circ - 275^\circ$ ). Both are very interesting seasons for the water cycle. The aphelion period, the coldest on Mars, is characterised by a strong hemispheric dichotomy, with a very dry south and a strong activity in the north induced by the onset and development of sublimation from the local polar cap, the biggest reservoir of water vapour for the planet. The second campaign, instead, allows to follow the water behaviour in a dustier and warmer environment (the campaign covers the moment of perihelion at  $L_s \sim 250^\circ$ ) and to analyse the onset of sublimation from the southern polar cap and the eventual differences with

respect to the northern one. Both campaigns cover mainly the mid-latitudes, but there are few profiles probing the polar regions and, especially during the second campaign, the northern tropic.

### Comparison with GCM predictions:

One of the main objectives of the study is to compare the retrieved profiles with those resulting from the LMD-GCM. As an example, Figure 2 shows the comparison for the northern hemisphere during the first MY29 campaign.

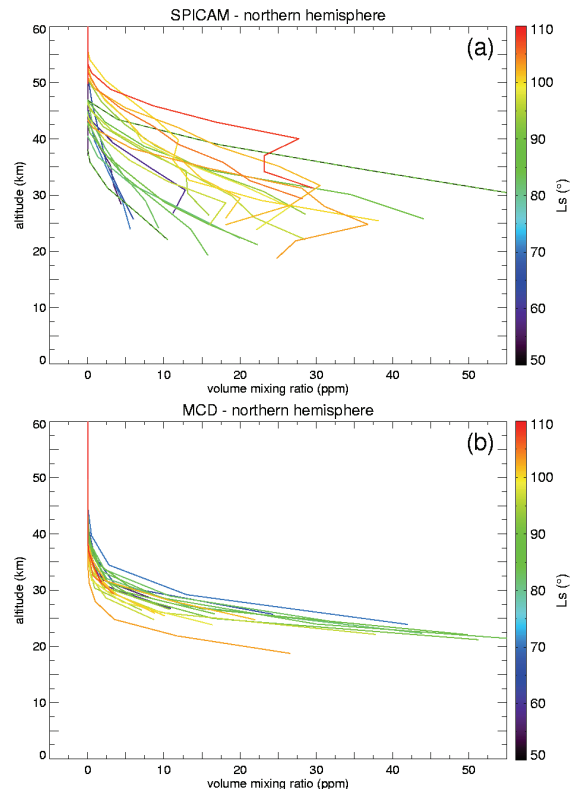


**Figure 2:  $\text{H}_2\text{O}$  volume mixing ratio profiles of the northern hemisphere for the first MY29 campaign. (a) SPICAM; (b) LMD-GCM. The colour indicates the day ( $L_s$ ).**

The results reveal important discrepancies. The measured profiles show a variety of shapes, and not just the regular exponential decline of the model. The presence of detached layers enriched in water, of up to 10 ppmv with respect to a regular smooth trend, is not uncommon (Figure 2 shows several examples especially after  $L_s = 100^\circ$ ).

The other major difference is the systematic detection of water vapour at significantly higher altitudes than the GCM. In the case illustrated by Figure 2, this effect is evident between 35 – 50 km, with a water excess of up to 25 ppmv with respect to the GCM. This has important consequences for water physics in the Martian atmosphere.

### Supersaturation in Martian atmosphere:

Supersaturation, which is a major factor for cloud formation on Earth's upper troposphere, is not allowed to exist in the climatologic models of Mars. Any amount of water exceeding the vapour pressure abundance is immediately converted into ice as if it instantaneously sediments. So, water vapour above the hygropane is never allowed to exceed the vapour pressure and falls rapidly towards negligible values, as a consequence of the decrease of temperature that generally prevails above 10 km. The detection by SPICAM of significant concentrations of water vapour in the layers above the hygropane, as defined by the temperature structure of the GCM, casts this assumption into question.

We computed the saturation ratio for the retrieved profiles, using the Goff-Gratch equation to deduce the corresponding vapour pressure in equilibrium over ice and the temperature profile from MCD. Results from the first occultation campaign show not only that water supersaturation exists in the Martian atmosphere, but also that it occurs frequently, in more than 50% of the orbits. The degree of supersaturation is significant: 25% of the orbits of the sample have a saturation ratio greater than 10. Figure 3 indicates how many Kelvin you have to add to the MCD temperature profile of each orbit in order to get the full orbit subsaturated. This allows to test the robustness of the detection with respect to the nominal model temperature uncertainty, which is  $\sim 5$  K. Indeed, in many cases more than 10 K must be added to the thermal profile to subsaturate the orbit, up to almost 20 K at the end of the campaign. Figure 3 also shows that supersaturation seems to follow a seasonal trend, with a minimum between  $L_s = 70^\circ - 80^\circ$  and the maximum values at the end of the campaign, after  $L_s = 100^\circ$ .

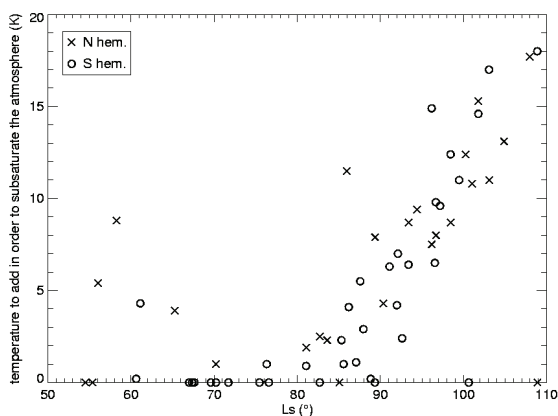


**Figure 3: temperature that must be added to the model temperature profile in order to subsaturate the atmosphere for each orbit of the first MY29 occultation campaign. Southern profiles are marked by circles and northern ones by crosses.**

The existence of supersaturation can be explained by a lack of efficiency of the condensation process, probably due to the lack of a sufficient number of condensation nuclei. In the absence of nuclei, the threshold saturation ratio for homogeneous nucleation exceeds 1,000.

### Dust-water interactions:

It is expected that the three main climatic cycles of Mars ( $H_2O$ ,  $CO_2$ , and dust) are intertwined in a complex manner and mutually influence each other with feedback processes. However, direct evidence of this kind of interaction is rarely observed. The vertical profiling of the atmosphere is a well-suited diagnostics to investigate this important feature of the Martian climate, and indeed the SPICAM dataset shows several unprecedented examples of the connection between the dust and the water cycle.

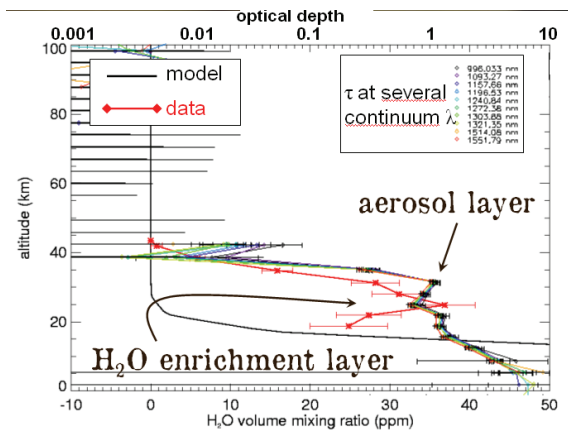


**Figure 4: a water-enriched layer often appears associated with an aerosol layer few km above. The black solid line is the water vapour mixing ratio predicted by the LMD-GCM. The red points united by a solid line, with error bars, show the retrieved  $H_2O$  mixing ratio. The series of coloured curves with similar shapes presents the optical depth at the various reference wavelengths.**

In many cases, a detached water layer is observed simultaneously with the presence of a detached aerosol layer. Interestingly, the water enriched layer appears always few kilometres below the aerosol one (Figure 4). This can be explained by microphysical phenomena associated with clouds. Water vapour first condenses within the aerosol layer. The resulting ice crystals then fall due to the action of gravity and consequently evaporate, creating the enriched vapour layer.

The reaction between water and dust seem to be a very rapid process. This is clearly seen in Figure 5, which shows the results from two orbits at high northern latitudes just after the northern summer

solstice. Only one Martian day separates them, but they exhibit a sudden jump in water vapour concentration, almost tenfold above 30 km. The two orbits have very similar temporal and spatial coordinates and thus very similar physical conditions, but between them an upsurge in dust activity happens (seen by the increase of the optical thickness of the atmosphere, bottom panel of Figure 5). Given that dust loading is the only difference between the two orbits, it can be safe to assume that the sudden variation of water concentration in the atmosphere is related to this dust event. Such an abrupt reaction suggests that the two cycles are more tightly connected than commonly believed.

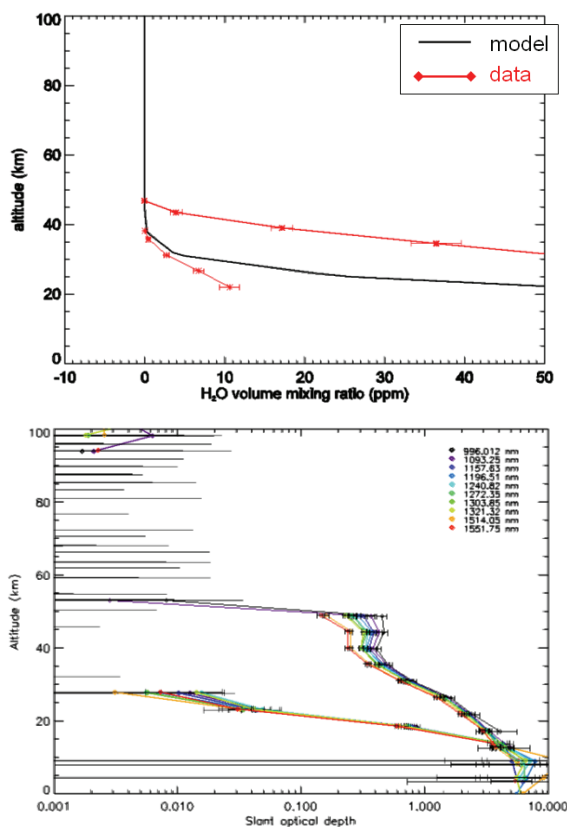


**Figure 5:** the sudden increase in water vapour concentration between orbit 5714 ( $L_s = 85^\circ$ ,  $59.1^\circ$  N –  $100.1^\circ$  E) and orbit 5721 ( $L_s = 86^\circ$ ,  $58.6^\circ$  N –  $119.1^\circ$  E), seen in the top panel, is mirrored by a surge of dust activity (represented by the optical depth of the bottom panel).

### Summary:

The SPICAM dataset of solar occultations allows an unprecedented look at the vertical behaviour of the water cycle. The vertical knowledge of water is essential to fully understand the mechanisms that underline the water cycle, and even if the dataset is still only partially analysed, it already shows important insights and trends, often not included in the most state-of-the-art climatologic models. Globally,

the results point at a tighter interaction between the main climatic cycles, especially dust and water, than previously expected. This is demonstrated by the enhanced importance that must be attributed to microphysical processes, which generate and rule the presence of supersaturation in the atmosphere, and by the fast reaction of water to the onset of dust events.

Future work will involve the elaboration of the full dataset, that will allow to extract a more complete picture of these phenomena and study in more detail their seasonal and interannual variations.

### References

- D.W. Davies, The vertical distribution of Mars water vapor, *J. Geophys. Res.* **84**, 2875 (1979).
- A. Fedorova et al., Solar infrared occultation observations by SPICAM experiment on Mars-Express: Simultaneous measurements of the vertical distributions of  $H_2O$ ,  $CO_2$  and aerosol, *Icarus* **200**, 96 (2009).
- F. Forget et al., Improved general circulation models of the Martian atmosphere from the surface to above 80 km, *J. Geophys. Res.* **104**, E10, 24155 (1999).
- T. Fouchet et al., Martian water vapor: Mars Express PFS/LW observations, *Icarus* **190**, 32 (2007).
- V.A. Krasnopolski, Photochemistry of the martian atmosphere: Seasonal, latitudinal, and diurnal variations, *Icarus* **185**, 153 (2006).
- F. Lefevre et al., Heterogeneous chemistry in the atmosphere of Mars, *Nature* **454**, 971 (2008).
- L. Maltagliati et al., Observations of atmospheric water vapor above the Tharsis volcanoes on Mars with the OMEGA/MEx imaging spectrometer, *Icarus* **194**, 53 (2008).
- E. Millour et al., The Latest (Version 4.3) Mars Climate Database, Third International Workshop on The Mars Atmosphere: Modeling and Observations, held November 10-13, 2008 in Williamsburg, Virginia. LPI Contribution No. 1447, 9029 (2008).
- F. Montmessin et al., Origin and role of water ice clouds in the Martian water cycle as inferred from a General Circulation Model, *J. Geophys. Res. (Planets)* **109**, E10004 (2004).
- M. Richardson et al., Water ice clouds in the Martian atmosphere: GCM experiments with a simple cloud scheme, *J. Geophys. Res. (Planets)* **107**, 5064 (2002).
- A. Rodin et al., Vertical distribution of water in the near-equatorial troposphere of Mars: water vapor and clouds, *Icarus* **125**, 212 (1997).
- L.S. Rothman et al., The HITRAN 2004 Molecular Spectroscopic Database, *J. Quant. Spectrosc. Radiat. Transf.* **96**, 139 (2005).
- H. Spinrad et al., The detection of water vapor on Mars, *Astrophys. J.* **137**, 1319 (1963).
- M. Tschimmel et al., Investigation of water vapor on Mars with PFS/SW of Mars Express, *Icarus* **195**,

557 (2008).